Int J Legal Med (2011) 125:493–502
DOI 10.1007/s00414-010-0444-6

ORIGINAL ARTICLE

Histomorphometric estimation of age in paraffin-embedded ribs: a feasibility study

Catherine Cannet · José Pablo Baraybar · Maryelle Kolopp · Pierre Meyer · Bertrand Ludes

Received: 15 November 2009 / Accepted: 8 March 2010 / Published online: 6 April 2010
© Springer-Verlag 2010

Abstract Estimation of age at death from human bones in legal medicine or in anthropology and archaeology is hampered by controversial results from the various macroscopic and histological techniques. This study attempted an estimation of age at death by histomorphometric analysis, from the fourth left rib adjacent to the costochondral joint in 80 forensic cases. Use of the picrosirius dye provided a reliable staining of the decalcified paraffin-embedded ribs. The total bone cortical area, the major and minor diameter as well as the area of the Haversian canals, the osteon areas of intact and remodelled secondary osteons, the area of non-Haversian canals were evaluated by means of image analysis, and derived parameters were calculated on both the internal and external sides of the rib. Most of the variables exhibited consistency between three different observers. Noteworthy, morphometric measurements in the internal cortex of the rib showed less variability than in the external cortex. Finally, discriminant statistical analysis from the 80 cases in this study indicated that the osteon population density was virtually sufficient to significantly discriminate between three groups of age: 20-39 (adulthood), 40-59 (middle age) and a group superior to 60. A subsequent blind evaluation of ten new subjects satisfactorily classified seven subjects out of ten within the three age groups. These results make feasible a larger study aimed at characterization of the practical relationships between bone tissue histomorphometry in ribs and chronological age in forensic cases.

Keywords Histomorphometry · Paraffin · Picrosirius · Rib internal cortex · Age at death · Discriminant analysis

C. Cannet (✉) · J. P. Baraybar · M. Kolopp · B. Ludes
Institut de Médecine Légale,
11 rue Humann,
67085 Strasbourg Cedex, France
e-mail: catherine.cannet@wanadoo.fr

P. Meyer
Laboratoire de Biostatistique, Faculté de médecine,
11 rue Humann,
67085 Strasbourg Cedex, France

Introduction

In legal medicine, anthropology or in archaeology, estimation of the age at death in human bones is essentially based on macroscopic examination. Dental criteria [1–3], cranial sutures [4–6], pelvic structure [7], morphology of the sternal end of the fourth rib [8] or radiological expertise [9] represent classical methods. There are also microscopic methods using histological analysis of the Haversian systems [10–33], as well as chemical determinations based on racemization of aspartic acid in dentine [34–36], in enamel [37] or in rib cartilage [38]. These approaches finally provided data with a broad variability, which led to controversies in age estimation [39]. Such a variability, which may extend from roughly 3-12 years, or more, has been explained by numerous factors: for example intra- or inter-observer variability, location of the sampling, differences in the techniques, choice of the studied bone, natural variations in the biological ageing or the critical choice of an adequate statistical analysis.

In this study, we attempted an estimation of age at death by histomorphometric analysis of paraffin-embedded ribs. The microscopic determination of age at death makes use of the continuous lifelong bone remodeling. Remodeling results from coupled resorptive and osteogenic events supporting the calcium homeostasis and the repairing of damaged or aged bones. In the cortex of long bones,

osteoclasts (bone-resorbing cells) and osteoblasts (bone-forming cells) are combined in the so-called basic multicellular units (BMUs) [40]. The end result of a BMU activity is the Haversian system or osteon.

Kerley [17] was the first author to use the life cycle of cortical bone in the estimation of age at death, by means of cross-sections of undecalcified long bone diaphysis (femur, tibia and fibula). The bone sections were performed through manual grinding of the undecalcified bone. The technique provides, however, uneven section thickness leading to unreliable histomorphometrical analyses [41]. Arguing that the technique was invasive and would prevent anthropologists to apply their standard osteometric analyses, Stout and Paine [27] developed a similar method to small bones, such as ribs and clavicles. In small bones, the cortical surface can be entirely evaluated, possibly avoiding under- or over-estimation of the histological features due to sampling location [12, 42]. The ribs are also believed to constitute a better sampling location in histological studies as they are less prone to biomechanical variations than long bones. The long bones are mainly involved in weight-bearing loads possibly providing a large variability in bone remodelling. In contrast, the repetitive stress arising from respiration is similar in humans [14].

Here, we developed a histomorphometrical evaluation based on the picrosirius staining of decalcified bone from forensic cases, namely a bone segment taken from the fourth left rib adjacent to the costochondral joint. The study was focused on: (1) the validation of a paraffin-embedded technique of decalcified rib to get a reproducible thickness of bone sections, (2) the search for a reliable definition of the microscopic structures in order to reduce the inter-observer differences, (3) the exploration of potential differences in the microscopic bone organisation between the internal and the external sides of the rib, as histomorphometric variations have been already observed in long bone sections, (4) the identification of cortical microscopic structures related to age, which would reduce the number of the measurements to one rib side because histomorphology may be very time-consuming and (5) the a priori prediction of age at death in a new set of subjects based upon the present experimental data to validate the whole process.

Materials and methods

Subjects

Left ribs were obtained from 80 forensic cases (62 males and 18 females) processed at the Institute for Forensic Medicine (Strasbourg, France) under the written agreement of the prosecutor. The names were also coded to preserve confidentiality. All subjects were Caucasian individuals, of known age and cause of death (Table 1). As evaluated from patient records and/or autopsy, none had a history of bone pathology. The age in male ranged from 20 to 91 years (mean±standard deviation: 57.6±20.0) and the age in female ranged from 20 to 70 years (42.2±12.0). An additional group of ten other new subjects (seven males and three females in the same conditions as mentioned above) were subsequently taken with blinded age labels to assess the statistical procedures.

Sample preparation

At autopsy, the sternal part of the fourth left rib adjacent to the costochondral joint was cut by saw in order to obtain a 3-4 cm bone segment. After removal of the intercostal muscles, the samples were fixed in 10% neutral buffered formalin for at least 7 days and then rinsed in running tap water for 6 h.

A 1 cm long transverse section, located distally to the chondrosternal end, was removed by saw and defatted in acetone for 5-7 days. This piece of bone was cleaned from residual soft tissues and periosteum, and decalcified in a mixture of 10% hydrochloric acid, 10% formic acid (*V*/*V*) for 5-8 h. After decalcification, the samples were trans-

Table 1 Causes of death and number of subjects

Cause of death	Number of subjects	Cause of death	Number of subjects
Aneurism	1	Blunt force injuries	3
Carcinoma, lung	6	Drowning	2
Carcinoma, urinary bladder	1	Drug-induced death	12
Cardiac arrest/myocardial infarction	23	Firearms injuries	4
Cerebral haemorrhage	2	Hanging	4
Severe pulmonary infection	10	Sharp force injuries	5
Pancreatitis	1	Fire and CO poisoning	3
Pulmonary embolus	5	Unknown	8

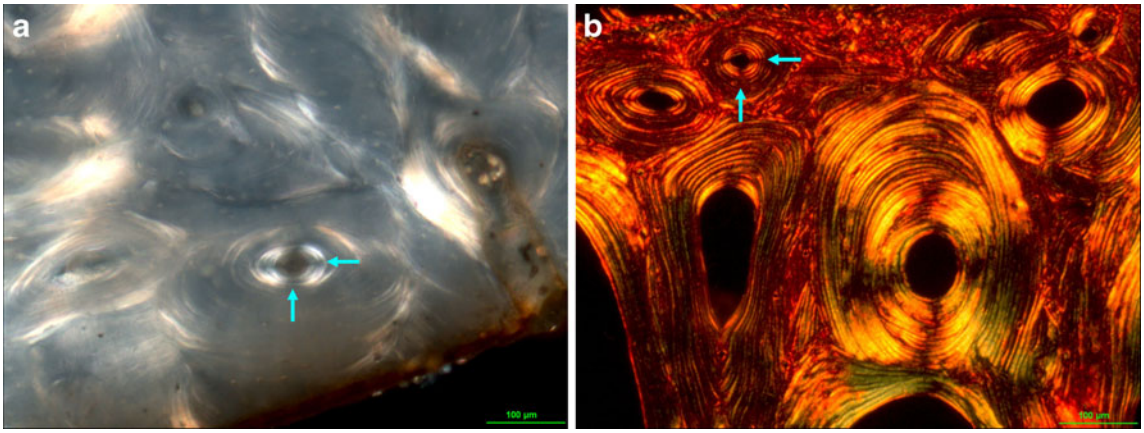

Fig. 1 **a** Undecalcified ground section, approximately 50 µm thickness, unstained, polarisation. **b** Decalcified bone section, 6 µm thickness, picrosirius stained, polarisation. Note the characteristic Maltese crosses (*arrows*) generated by the concentric lamellae of osteons and the more contrasted picture (**b**) of the decalcified picrosirius stained bone when compared to the calcified unstained bone (**a**)

versally halved in two segments, dehydrated through increasing graded series of ethylic alcohol, cleared in xylene and both segments were finally embedded in the same paraffin block. Paraffin with a high melting point of 62-64°C was retained to provide a more solid matrix to the bone and consequently an easier sectioning. The internal parts of the ribs were systematically placed on the side of the identification number of the embedding cassette. Tissue sections of 6 µm in thickness were stained with the picrosirius red method [43, 44] using Sirius red F3B (C.I. 35782) as a dye.

The main feature under polarisation of undecalcified cortical bone is the Maltese cross, which is generated by the concentric lamellae of Haversian system. The same aspect is observed even after decalcification of the bone (Fig. 1a and b). This typical Maltese cross-pattern is due to the orientation of collagen fibres bundles. Within the same lamella, collagen fibres are predominantly parallel to one another and have a preferred orientation within the lamellae. The orientation of collagen fibres between lamellae may change up to 90° in adjacent lamellae [45, 46]. The polarisation of bone depends on the orientation of collagen fibres due to their birefringency [47]. Bone matrix is composed of 90% of collagen I fibres. During bone formation, collagen molecules of the osteoid matrix aggregate and form fibrils of precise three-dimensions structures. Space within fibrils, often referred to as "hole zones", provides initiation sites for the calcium-phosphate crystals deposition (apatite crystals). Bone apatite crystals are always deposited in such a way that their longest dimension lies parallel to the axis of the collagen fibrils [48, 49]. Sirius red F3BA allows a collagen-specific staining which differentiates between collagen fibres I, III and IV, when observed under polarised light [43, 44]. The elongated dye molecules are attached parallel to the collagen fibres resulting in an enhanced birefringency. This method provides highly contrasted pictures for the observation and the quantification of the micro-architecture of the bone [50].

Image capture

The internal and external cortices of each rib were captured at ×5 magnification, using a microscope (Axiophot, Zeiss) equipped with differential interference contrast and connected to a digital video camera (DFC 420, Leica). Six to ten contiguous pictures per rib side were captured; the first and the last pictures were located 1-2 mm from the superior or inferior rib border (Fig. 2). Internal and external cortical pictures were coded at the time of image capture to allow a blind assessment of the microscopic structures. Histomorphometric analyses were performed using the "Image Manager" Software (IM 500, Leica) and the measured values were automatically transferred to an Excel table for further calculations.

Description of the histological structures

The three histological structures chosen in this study (Figs. 3 and 4) were adapted from the Kerley's and Thompson's descriptions [17, 29]:

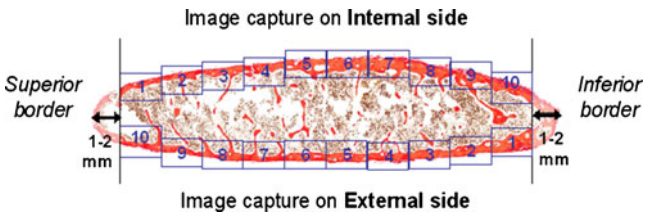

Fig. 2 Description of image capture

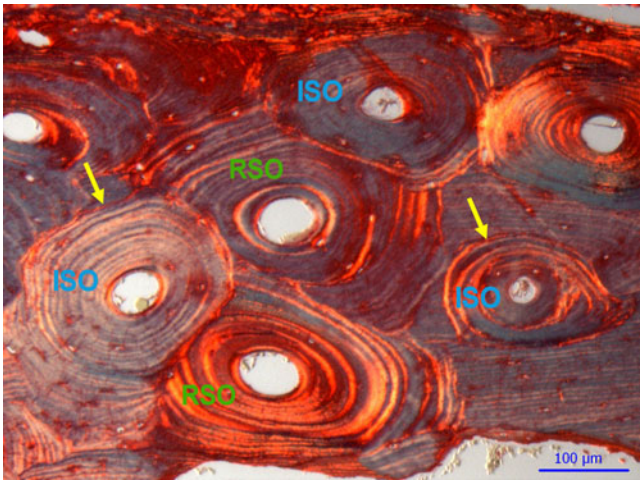

Fig. 3 Description of intact secondary osteons (ISO) and remodelled secondary osteons (RSO). Intact secondary osteons (ISO) were circular structures, surrounded by a cement line (*arrow*) and formed by concentric lamellae around an intact Haversian canal. In our study, osteons having at least 80% of their reversal line unremodelled were considered as ISO. *Remodelled secondary osteons (RSO)* were intact secondary osteons having more than 80% of their reversal line remodelled. The Haversian canal had to be identifiable. Remodelled secondary osteons lacking Haversian canal were excluded from the counting. This underestimated fragmentary osteons but avoided a possible confusion with interstitial lamellae [56]

Measurements

Direct measurements

The following structures were manually delineated on each picture. The histomorphometric features were expressed in micron metre (µm) for linear measurements, and square micron metre (µm^2) for areas.

1. *Total bone cortical area (TCAr):* i.e. the bone contained between endosteum and periosteum, with the exclusion of any remaining soft tissue, trabecular bone and any incomplete cavity located on the lateral side of the picture (Fig. 5),
2. *Major diameter (MD) and minor diameter (mD) of the Haversian canal* in intact secondary osteons (ISO) and remodelled secondary osteon (RSO), when 80% of the reversal line was on the picture. The two criteria for this measurement consisted in: (1) the major diameter was not larger than 2.5 times the minor one; (2) the major diameter was inferior to 150 µm. Canals that did not fit these criteria were considered as non-Haversian's canals,
3. *Haversian canal area (HCAr):* surface of Haversian canal, when 80% of the reversal line was contained within the picture,
4. *Osteon area of non-remodelled osteon (OAr)*: surface of intact secondary osteon circumscribed by the reversal line, when 80% of the reversal line was contained within the picture,
5. *Area of non-Haversian canal*: surface of Volkmann's canals and resorption spaces.

Derived calculations

All derived values, for each internal and external rib side, were calculated by using Excel (Windows, version 2003):

1. *Mean total bone cortical area (CAr)*: sum of all CAr divided by the number of pictures, per side (internal or external),
2. *Compact cortical bone area (CoCAr)*: sum of all CAr values minus sum of all NoHAr values,
3. *Number of ISO and of RSO*: counted according to the number of Haversian canals, for ISO and RSO, respectively,
4. *Osteon population density (OPD):* number of (ISO+ RSO) divided by CoCAr, per square millimetre,

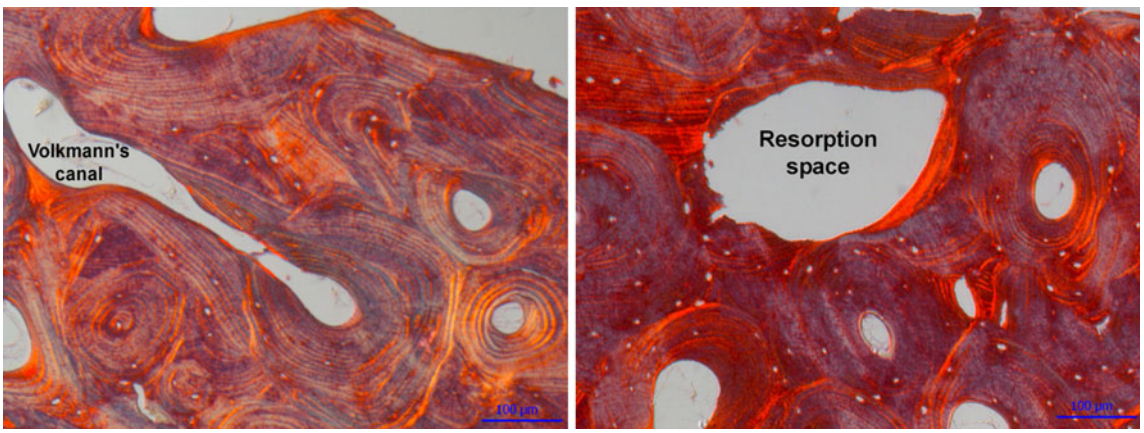

Fig. 4 Description of non-Haversian canals. Non-Haversian canals (NHC) corresponded to all spaces not surrounded by a cement line such as the Volkmann's canals and the resorption spaces. Large non-Haversian canals may be lined by one or two layers of concentric lamellae

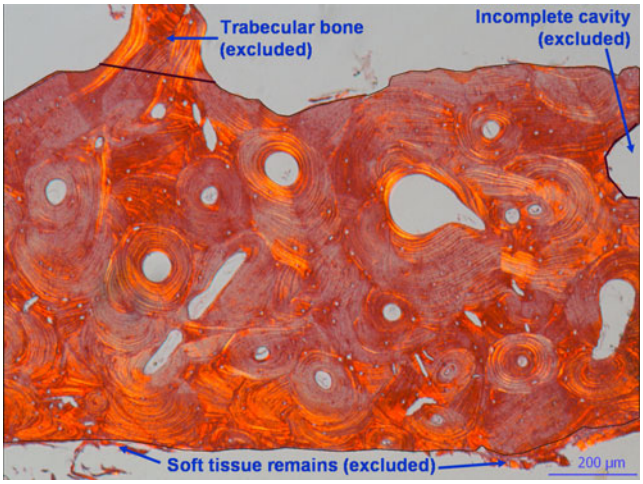

Fig. 5 Description of total bone cortical area delineation

5. *Haversian canal density (HCaD):* sum of HCAr divided by CoCAR, reported per square millimetre,
6. *Non-Haversian canal density (NoHCD):* sum of non-Haversian canal area divided by CoCAr, reported per square millimetre.

Statistical analysis

Data were expressed as means±standard deviations. As the measured variables were normally distributed (assessed with the Kolmogorov-Smirnov test), we used the two-tailed paired *t* test to compare data between the internal and the external cortices, i.e. the cortical area, the osteon population density, the mean osteon area, the Haversian canal density and the non-Haversian canal density. Otherwise a two-tailed unpaired *t* test was used. Calculations of the linear regressions were made by using the Excel® functions. The statistical significance was conventionally evaluated at: $p<0.05$, $p<0.01$, $p<0.001$.

Characterization of the relationships between age and morphometric data was attempted trough conventional regression analysis and then performed by using an analysis of variance and a discriminant analysis. Discriminant analysis was retained because it allows classification of subjects into separated classes with a predefined probability (usually $p<0.05$) as compared to regression analysis which allocates a subject on a linear regression line, usually within a large ellipse of confidence (here $r^2=0.504$ at $p<0.05$; data not shown). The SPSS-14 and Minitab statistical packages were used.

The so-called discriminant analysis has been developed by Fisher [51, 52]. It is a statistical technique used for classifying a set of observations into predefined classes. The purpose is to determine the class of an observation based on a set of variables known as predictors or input variables. The model is based on a set of observations for which the classes are known. This set of observations is sometimes referred to as the training set. Based on this training set, the technique constructs a set of linear functions of the predictors known as discriminant functions. These discriminant functions are then used to predict the class of a new observation.

In the first training step, we used 80 cases with known ages. Calculation retained one histomorphometric parameter, i.e. a variable (it might have been more than one), which significantly (at $p<0.05$) distinguished between three groups of age (adulthood, middle age and superior to 60: it might have been more than three). In the second step, we took ten other new cases in which the age labelling was blinded, and then we applied the above-mentioned trained model to classify these ten new cases into the three defined groups of age (at $p<0.05$). Removal of the labels showed how many among the ten subjects were correctly classified within the three groups of age.

Results

Comparison of histomorphometric analysis between the internal and external cortices

The mean cortical area (CAr), which expressed the amount of bone tissue within a given histological piece, was found to be significantly thicker ($p<0.05$) in the internal cortical side than in the external one by a factor of 14%. The other parameters, such as OPD, HCaD, non-Haversian canal density (NoHCD) and mean area of intact secondary osteon showed no significant differences ($p>0.05$) between the internal and external sides (Table 2).

Visual observation of bone sections showed that the shape of the Haversian canals usually appeared to be more

Table 2 Differences of CAr, OPD, OAR, HCaD and NoHCD between the internal and external sides of the rib

Rib side (n=80)	Mean cortical area CAr [µm^2] *	OPD (Nb/mm^2)	Mean area osteon OAr [µm^2]	Haver's canal density HCaD [µm^2/mm^2]	No Haver's canal density NoHCaD [µm^2/mm^2]
Internal	615 043±263 877	12.5±3,7	15 087±5 748	16 295±4 438	42 115±23 647
External	525 746±219 159	12.1±3,4	14 790±5 029	15 801±5 121	33 980±31 998

Mean±SD, unpaired *t* test, *$p<0.05$

ovoid than round. This possibly reflects an asymmetric process of bone remodelling between resorption and absorption during BMUs activity. Thus, the major and minor diameters of each Haversian canal were evaluated to attempt a quantification of potential differences in remodelling between the internal and external sides of the ribs.

A ratio in the major/minor (M/m) diameters above 1.50 visually corresponded to a definite ovoid-shape-like of the canal. According to this classification, 67%±13% of the total number of canals in the internal cortex exhibited a major diameter 1.50 superior to the minor one. When compared to the 58%±17% in the external cortex, the difference was found to be significant (unpaired t test $p<0.001$).

In addition, the coefficient of variation ($\sigma/\mu=0.20$) within the internal cortex was found to be twice as high within the external one (0.40). Hence, morphometric variations of the Haversian canals were less pronounced within the internal side than the external one.

Inter-observer analyses

The histomorphometric evaluations were performed by three different observers on randomly chosen 13 ribs. The total cortical area, the number of ISO and RSO, the area of Haversian canals and area of non-Haversian canals were evaluated in a blind manner. Age at death was unknown and the observers performed independent observations. Observer A was a trained histologist with experience in histomorphometry, observer B was a trained anthropologist with no experience in histology and observer C was a trained forensic pathologist with experience in microscopic anatomic pathology.

On one hand, the coefficients of correlation r^2 were calculated from the linear regression analysis of the data obtained by the three observers within seven parameters (Table 3, observer A vs. observer B, and conversely A and C, B and C). On the other hand, the mean values of the same seven parameters were statistically compared between the three observers (Table 3).

A high coefficient of correlation is coupled with an absence of statistical difference between the three observers within the main parameters, the total number of osteons (ISO+RSO), the osteon population density and the total cortex area. The difference appeared to be significant in the case of ISO and RSO, when counted separately, and in the case of the Haversian canal density. In fact, only one observer was responsible for this discrepancy, and the two other ones were in complete agreement.

The data resulting from measurements of the total cortical area, ISO, RSO, the sum of ISO+RSO, OPD, the sum of Haversian canals and of the non-Haversian canals were also visualised by a series of scatter plots. For each parameter, values were plotted against each observer (A versus B, A vs. C and B vs. C) including a line of equality, i.e. a line on which all points should lie in case of complete agreement between observers [53] The agreement between the three observers was particularly striking in the case of the OPD (1 in Fig. 6) but less consistent in the case of the total RSO per rib, a parameter exhibiting discrepancies due to one observer (2 in Fig. 6).

Estimation of age at death

Mining the data by analysis of variance and discriminant analysis (see "Materials methods" section), indicated that the OPD within the internal cortex appeared to be one of the most reliable to classify the individuals. The other variables improved only marginally the classifications. In this feasibility study, the three age groups were chosen as the result of a compromise between the number of items per group to get a satisfactory statistical significance and the biological constraints (Table 4). According to Iscan MY [8], the rib morphology is more variable after the age of 39. Thus, the first group (adulthood) ranged here between 20 and 39. The two other groups were rather arbitrary chosen between 40 and 59 (middle age) and superior to 60. The number of subjects in each group was respectively: 22 (first group), 26 (second group) and 32 (third group). There were

Table 3 Linear regression analysis (r^2) and statistical evaluation (paired t test) of the potential differences between the three observers within seven histomorphometric parameters

	Observer A vs. B		Observer A vs. C		Observer B vs. C	
	r^2	p	r^2	p	r^2	p
Total ISO per rib	0.7226	-***	0.9319	NS	0.5717	-***
Total RSO per rib	0.3795	-***	0.8764	NS	0.5091	-***
Total ISO+RSO per rib	0.9910	NS	0.9851	NS	0.9970	NS
OPD	0.9920	NS	0.9883	NS	0.9918	NS
Total cortical area (mm^2)	0.9939	NS	0.9895	NS	0.9977	NS
Haversian canal density (μm^2 x10^3)	0.7492	-**	0.8639	NS	0.5131	-***
Non-haversian canal density(μm^2 x10^3)	0.8756	NS	0.8710	NS	0.7964	NS

NS non-significant

**$p<0.01$; ***$p<0.001$

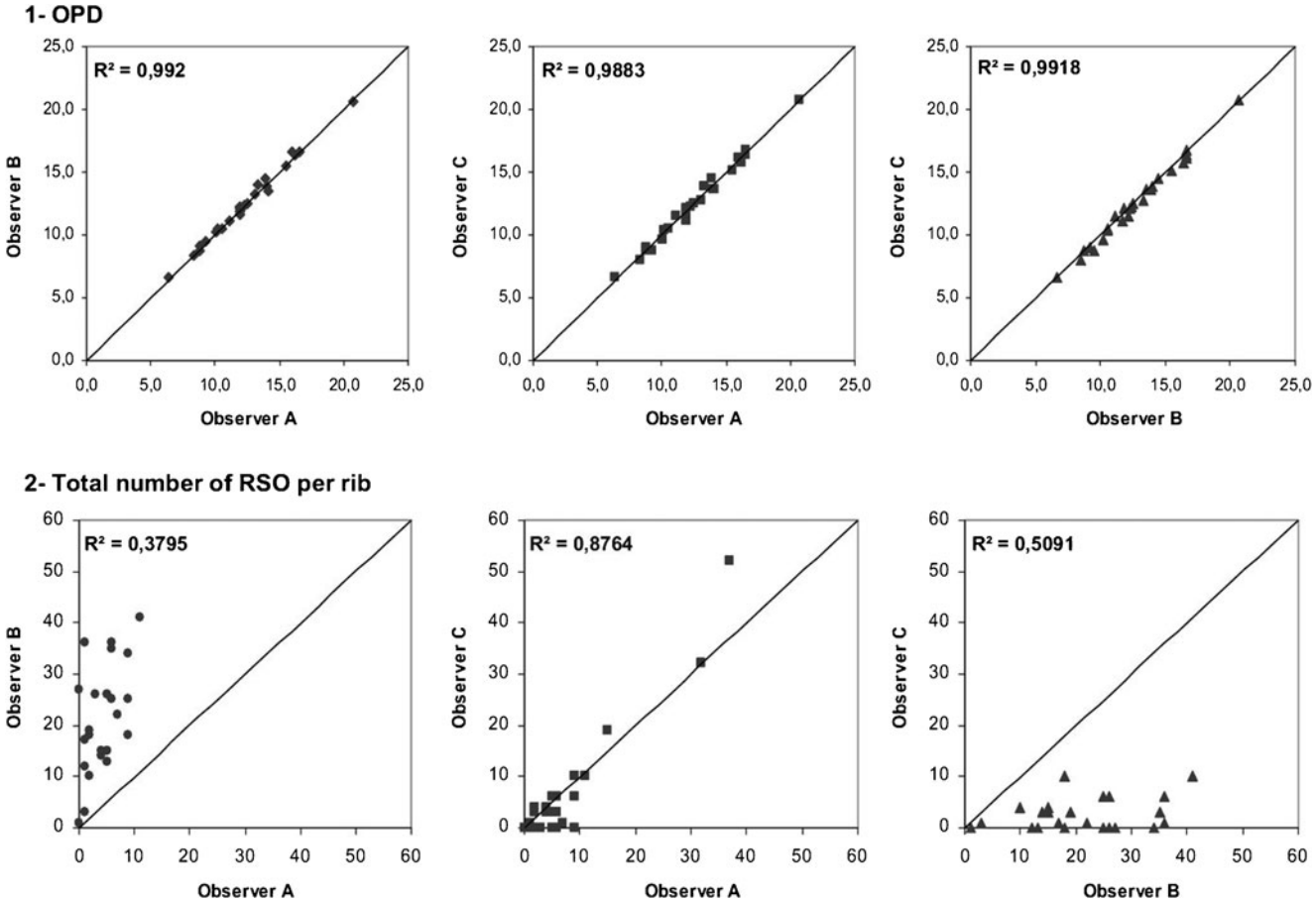

Fig. 6 Scattered plots from OPD (*1*) and total RSO per rib (*2*) between the three different observers (A, B and C)

not enough subjects per group to statistically distinguish between four or more groups of age.

The classification Fisher discriminant function, calculated from the series of 80 individuals with OPD as the only variable, respectively provided 77.3%, 57.7% and 71.9% of correct classification ($p<0.05$) into the three groups of increasing age which have been previously defined. This training phase was then used to classify the ten new subjects within the three age classes. Uncovering the age labels showed that seven out of ten individuals were correctly classified at $p<0.05$.

Table 4 Mean, SD and confidence interval at $p<0.05$ of the OPD in the internal cortex, per age classes

Age classes	Mean±SD	Confidence interval
20-39 (n=22)	8.64±2.94	7.34-9.95
40-59 (n=26)	12.49±2.38	11.53-13.46
>=60 (n=32)	15.26±2.49	14.36-16.15

Discussion

Gender and age are important parameters for the identification of human skeletal remains. Thanks to DNA analyses, it is usually easy to achieve sex determination but evaluation of the age at death often provides variable data. It was first attempted to assign the age of cadavers from gross-anatomical characteristics. Criteria appeared to be rather accurate below 40 but become vague after this age. In addition, these macroscopic methods cannot be applied to fragmentary skeletal remains. Thus, histological techniques were tentatively used in the estimation of age at death, first on long bones then on small bones like ribs and clavicles, in order to investigate the whole cortical surface.

The reference technical preparation of bone section is a manual grinding of undecalcified bone, either resin-embedded or not. Thickness of the bone sections varies among authors from 50 to 200 μm. The technique is time consuming, generates bone dust (especially in case of dry bone) and finally provides an uneven thickness from one section to another and also within the same section. Recent

attempts to reduce the thickness and the time of preparation [54] did not improve reproducibility in the sections thickness. A manual grinding still precludes evaluations on serial sections and bone section thickness is a critical parameter for histomorphometric analyses [41]. The alternative is to embed bone in a resin medium with the disadvantage of working with toxic chemicals and expensive equipment.

A paraffin method applied to decalcified ribs was first validated by Telmon, after a comparison of data obtained from calcified and decalcified ribs [55]. The method is cheap and adaptable to a routine laboratory work. It allows the processing of numerous samples in a short time with a reproducible thickness. As different staining may be done on serial sections, this might be of value for diagnosis. Embedding in paraffin needs a previous decalcification of the bone. A solution combining weak and strong acids, the formic and hydrochloric respectively, achieved decalcification within a reasonable timeline and without distortion in the microstructure. Decalcification combined with picrosirius red staining and in conjunction with polarisation light, constitutes an indirect method for observation and quantification of the bone matrix micro-organisation.

A review of the literature showed that definition of the delineated structures for the histomorphometric analyses varies among the authors [56]. In a preliminary intra-observer analysis performed by a trained histologist (data not shown), some of the structures defined by previous authors [17, 29] were used, but did not result in reproducible counts in our hands, especially the ones concerning the fragmentary osteons and the lamellar bone. The most objective criteria were tested and finally retained after validation through an inter-observer study, according to the Schmitt's recommendations [57].

Significant variations in bone microstructures have been reported in long bone according to the sampling locations [42]. Moreover, bone remodelling and osteon density are known to be under the influence of factors like biomechanical stress, physical effort, nutrition or hormonal status [58]. The major biomechanical repetitive constraint within the ribs appears to be linked to the breathing [14]. Thus, we looked for potential differences in histological structures between the internal and external cortices of the rib. The internal cortical area was found to be significantly thicker than the external one in male and female. A possible explanation might be related to the sampling location closed to the costochondral joint. Indeed, among the muscles inserted on the rib external and internal sides, the pectoris minor muscle is the only one to exert a differential biomechanical stress limited to the external rib side. A similar difference (internal vs. external cortex) is to be expected within the sternal end of ribs 2 to 5-6, as the muscle insertions are similar.

Variation in the shape of the Haversian canals was found to be more pronounced in the external side. A technical artefact seems to be excluded, as a non-transverse section through the rib would affect both sides in the same way. A preferential orientation of the Haversian canals in the internal vs. the external rib side might explain it. Variation in the shape of Haversian canals in human ribs have been already described in the so-called "drifting osteons" [59], defined as osteons with eccentric canals showing elliptical forms when viewed in cross-sections. They are interpreted as the consequence of an asymmetric process of bone remodeling, between resorption and formation. The author postulated that some agent in the bone marrow cavity favours a negative cortical endosteal bone balance and that some agent at the periosteal surface favours a positive periosteal bone balance, or that both factors are involved. In our study, the M/m diameter ratio of Haversian canals >1.50 was highest in the external cortex. According to some authors [60, 61], this histomorphometric measurement correlated with an increased risk of fracture and could possibly bias microscopic analyses on external cortex. On one hand, the orientation of osteons was found to be less variable in the internal cortex and on the other hand, the internal cortex exhibited a larger area. This may explain why measurements of the OPD within the internal side appeared to be an important parameter for estimation of the age at death.

Inter-observer evaluations indicated that even with precise definitions in the histological structures to be delineated, the separate count of intact and remodelled osteons remained subjective for observers with no previous experience in histology. However, the lack of experience did not affect the final calculation of OPD. The total number of ISO and RSO, the non-Haversian canal density as well as the total cortical area, showed indeed no statistical difference between observers. The present study is in agreement with the other studies that considered OPD as the most reliable parameter for the histological determination of age-at-death [31, 53, 62, 63].

When considering unidentified cadavers or human remains, it was commented by Rösing and Kvaal [64] that methods with a standard error of more than 5-7 years were not suitable for routine forensic application, e.g. for estimating age at death. This means that a 95% confidence interval around ±14 years or more might have to be considered in age estimation [65]. In a critical review on the various methods used in the estimation of age at death [39], histology of the bone was recommended in cadavers and human remains of all ages, as well as in historic and archaeological cases. Variations of the methods were estimated by standard errors which ranged from 5 to 12 years, and the relationships between chronological age and the potential histological marker was often assessed by

linear regression analysis with coefficients of correlation from 0.68 to 0.90. This explains why it remains hazardous to infer a chronological age in a new individual case.

The discriminant analysis used in this feasibility study performed a fairly correct (i.e. at a statistical significance of $p<0.05$) classification of a series of ten new subjects. However, the present three age groups (adulthood, middle age and a group superior to 60) are clearly still too broad classes for practical applications, in forensic medicine for example. A statistically more robust classification would request a minimum of 30 subjects per age group. It is thus anticipated that a higher number of individuals might improve the number of significant groups of age, as far as the biological variability remains within the present boundaries of that study.

Conclusion

In this study, the present picrosirius technique and the histomorphometric parameters estimated in paraffin-embedded ribs provided standardised data. Statistical discriminant analysis, based on a training set of 80 cases and a test set of ten cases, provided a sound classification in three groups of age. This make feasible a larger study aimed at characterization of the practical relationships between bone tissue histomorphometry in ribs and chronological age in forensic cases.

References

1. Gustafson G (1950) Age determination on teeth. J Am Dent Assoc 41(1):45–54
2. Lamendin H, Baccino E, Humbert JF, Tavernier JC, Nossintchouk RM, Zerilli A (1992) A simple technique for age estimation in adult corpses: the two criteria dental method. J Forensic Sci 37 (5):1373–1379
3. Prince DA, Ubelaker DH (2002) Application of Lamendin's adult dental aging technique to a diverse skeletal sample. Forensic Sci 47(1):107–116
4. Perizonius WRK (1984) Closing and non-closing sutures in 256 crania of known age and sex from Amsterdam (AD 1883-1909). J Hum Evol 13:201–216
5. Todd TW, Lyon DW (1924) Endocranial suture closure. Part I: adult males of white stock. Am J Phys Anthropol 7:325–384
6. Todd TW, Lyon DW (1925) Ectocranial suture closure. Part II: adult males of white stock. Am J Phys Anthropol 8:23–43
7. Brooks S, Suchey JM (1990) Skeletal age determination based on the os pubis: a comparison of the Acsadi-Nemeskeri and Suchey-Brooks methods. Hum Evol 5:227–238
8. Iscan MY, Loth SR, Wrigh RK (1984) Age estimation from the rib by phase analysis: white males. J Forensic Sci 29(4):1094–1104
9. Krogman WM (1986) The human skeleton in forensic medicine. Charles C Thomas, Springfield
10. Ahlquist J, Damsten O (1969) A modification of Kerley's method for the microscopic determination of age in human bone. J Forensic Sci 14:205–212
11. Bouvier M, Uberlaker DH (1977) A comparison of two methods for the microscopic determination of age at death. Am J Phys Anthropol 46:391–394
12. Chan AHW, Crowder CM, Rogers TL (2007) Variation in cortical bone histology within the human femur and its impact on estimating age at death. Am J Phys Anthropol 132:80–88
13. Cho H, Stout SD, Madsen RW, Streeter MA (2002) Population-specific histological age-estimating method: a model for known African-American and European-American skeletal remains. J Forensic Sci 47(1):12–18
14. Crowder C, Rosella L (2007) Assessment of intra- and intercostal variation in rib histomorphometry: its impact on evidentiary examination. J Forensic Sci 52(2):271–276
15. Ericksen MF (1991) Histologic estimation of age at death using the anterior cortex of the femur. Am J Phys Anthropol 84(2):171–179
16. Ericksen MF, Stix AI (1991) Histological examination of age of the first african baptist church adults. Am J Phys Anthropol 85:247–252
17. Kerley ER (1965) The microscopic determination of age in human bone. Am J Phys Anthropol 23:149–163
18. Kerley ER, Ubelaker DH (1978) Revisions in the microscopic method of estimating age at death in human bone. Am J Phys Anthropol 49:545–546
19. Kim YS, Kim DI, Park DK, Lee JH, Chung NE, Lee WT, Han SH (2007) Assessment of histomorphological features of the sternal end of the fourth rib for age estimation in Koreans. J Forensic Sci 52(6):1237–1242
20. Maat GJR, Maes A, Aarents MJ, Nagelkerke NJD (2006) Histological age prediction from the femur in a contemporary dutch sample: the decrease of non-remodeled bone in the anterior cortex. J Forensic Sci 51(2):230–237
21. Mulhern DM (2000) Rib remodelling dynamics in a skeletal population from Kulubnarti, Nubia. Am J Phys Anthropol 111:519–530
22. Paine RR, Brenton BP (2006) Dietary health does affect histological age assessment: an evaluation of the Stout and Paine (1992) age estimation equation using secondary osteons from the rib. J Forensic Sci 51(3):489–492
23. Stout SD (1986) The use of bone histomorphometry in skeletal identification: the case of Francisco Pizarro. J Forensic Sci 31 (1):296–300
24. Stout SD (1988) The use of histomorphology to estimate age. J Forensic Sci 33(1):121–125
25. Stout SD, Dietze WH, Iscan MY, Loth SR (1994) Estimation of age at death using cortical histomorphometry of the sternal end of the fourth rib. J Forensic Sci 39(3):778–784
26. Stout SD, Gehlert SJ (1980) The relative accuracy and reliability of histological aging methods. Forensic Sci Int 15:181–190
27. Stout SD, Paine RR (1992) Brief communication: histological age estimation using rib and clavicle. Am J Phys Anthropol 87:111–115
28. Stout SD, Porro MA, Perotti B (1996) Brief communication: a test and correction for the clavicle method of Stout and Paine for histological age estimation of skeletal remains. Am J Phys Anthropol 100:139–142
29. Thompson DD (1979) The core technique in the determination of age at death in skeletons. J Forensic Sci 24(4):902–915
30. Thompson DD (1981) Microscopic determination of age at death in an autopsy series. J Forensic Sci 26(3):470–475
31. Thompson DD, Calvin CA (1983) Estimation of age at death by tibial osteon remodeling in an autopsy series. Forensic Sci Int 22:203–211
32. Watanabe Y, Konishi M, Shimada M, Ohara H, Iwamoto S (1998) Estimation of age from the femur of Japanese cadavers. Forensic Sci Int 98:55–65

33. Yoshino M, Imaizumi K, Miyasaka S, Seta S (1994) Histological estimation of age at death using microradiographs of humeral compact bone. Forensic Sci Int 64:191–198
34. Helfman PM, Bada JL (1976) Aspartic acid racemization in dentine as a measure of ageing. Nature 262:279–281
35. Ohtani S, Yamamoto K (1987) Age estimation using the racemization of aspartic acid on human dentin. Nihon Hiogaku Zasshi 41(3):181–190
36. Ritz S, Schütz HW, Peper C (1993) Postmortem estimation of age at death based on aspartic acid racemization in dentin: its applicability for root dentin. Int J Legal Med 105:289–293
37. Ohtani S, Ito R, Arany S, Yamamoto T (2005) Racemization in enamel among different types of teeth from the same individual. Int J Legal Med 119:66–69
38. Pfeiffer H, Mörnstad H, Teivens A (1995) Estimation of chronological age using the aspartic acid racemization method. I. On human rib cartilage. Int J Legal Med 108:19–23
39. Ritz-Timme S, Cattaneo C, Collins MJ, Waite ER, Schütz HW, Kaatsch HJ, Borrman HIM (2000) Age estimation: the state of the art in relation to the specific demands of forensic practice. Int J Legal Med 113:129–136
40. Frost HM (1963) Bone remodelling dynamics. Charles C Thomas, Springfield
41. Johansson CB, Morberg P (1995) Importance of ground section thickness for reliable histomorphometrical results. Biomaterials 16 (2):91–95
42. Pfeiffer S, Lazenby R, Chiang J (1995) Brief communication: cortical remodeling data are affected by sampling location. Am J Phys Anthropol 96(1):89–92
43. Junqueira LC, Bignolas G, Brentani RR (1979) Picrosirius staining plus polarization microscopy, a specific method for collagen detection in tissue sections. Histochem J 11(4):447–455
44. Puchtler H, Waldrop FS, Valentine LS (1973) Polarization microscopic studies of connective tissue stained with picro-sirius red F3BA. Beitr Pathol Anat 150:174–187
45. Ascenzi A, Bonucci E (1970) The mechanical properties of the osteon in relation to its structural organisation. In: Balazs EA (ed) Chemistry and molecular biology of the intercellular matrix. New York, Academic Press
46. Ascenzi A, Bonucci E (1976) Relationship between ultrastructure and "pin test" in osteons. Clin Orth Rel Res 121:275–294
47. Bromage TG, Goldman HM, Mc Farlin SC, Warshaw J, Boyde A, Riggs CM (2003) Circularly polarized light standards for investigations of collagen fiber orientation in bone. Anat Rec B New Anat 274(1):157–168
48. Johnson LR (2003) Essential medical physiology. Academic, London, pp 681–682
49. Young B (2006) Wheater's functional histology: a text and colour atlas, 5th edn. Churchill Livingstone, Edinburgh, pp 189–201
50. Dziedzic-Goclawska A, Rozycka M, Czyba JC, Moutier R, Lenczowski S, Ostrowski K (1982) Polarizing microscopy of picrosirius stained bone sections as a method for analysis of spatial distribution of collagen fibers by optical diffractometry. Basic Appl Histochem 26(4):227–239
51. Romeder JM (1973) Méthodes et programmes d'analyse discriminante. Dunod, Paris
52. Venables WN, Ripley BD (2002) Modern applied statistics with S. Springer, New York
53. Lynnerup N, Thomsen JL, Frohlich B (1998) Intra- and inter-observer variation in histological criteria used in age-at-death determination based on femoral cortical bone. Forensic Sci Int 91:219–230
54. Maat GJR, van den Bos RPM, Aarents MJ (2001) Manual preparation of ground sections for the microscopy of natural bone tissue. Update and modification of Frost's ''rapid manual method''. Int J Osteoarchaeol 11:366–374
55. Telmon N, Allery JP, Blanc A, Gainza D, Rougé D (2004) Comparaison de méthodes de détermination histologique et scopique de l'âge à partir de l'extrémité sternale de la 4ème côte. Antropo 7:203–209
56. Iwaniec TU, Crenshaw TD, Schoninger MJ, Stout SD, Ericksen MF (1998) Methods for improving the efficiency of estimating total osteon density in the human anterior mid-diaphyseal femur. Am J Phys Anthropol 107:13–24
57. Schmitt A (2002) Estimation de l'âge au décès des sujets adultes à partir du squelette: des raisons d'espérer. Bull et Mém de la Société d'Anthropologie de Paris, ns, t 14(1–2):51–73
58. Frost HM (1985) The "new bone": some anthropological potentials. Yr Physical Anthropol 28:211–226
59. Epker BN, Frost HM (1965) The direction of transverse drift of actively forming osteons in human rib cortex. J Bone Joint Surg Am 47A:1211–1215
60. Cormier J (2003) Microstructural and mechanical properties of human ribs. Thesis, University of Virginia
61. Pfeiffer S (1998) Variability in osteon size in recent human populations. Am J Phys Anthropol 106(2):219–227
62. Lynnerup N, Frohlich B, Thomsen JL (2006) Assessment of age at death by microscopy: unbiased quantification of secondary osteons in femoral cross-sections. Forensic Sci Int 159S:S100–S103
63. Stout SD, Stanley SC (1991) Percent osteonal bone versus osteon counts: the variable of choice for estimating age at death. Am J Phys Anthropol 86:515–519
64. Rösing FW, Kvaal SI (1997) Dental age in adults. A review of estimation methods. In: Alt KW, Rösing FW, Teschler-Nicola M (eds) Dental anthropology. Fundamentals, limits and prospects. Springer, Wien, pp 443–468
65. Giles E, Klepinger LL (1988) Confidence intervals for estimates based on linear regression in forensic anthropology. J Forensic Sci 33(5):1218–1222